



HAL
open science

Layer-sensitive magneto-optical Kerr effect study of magnetization reversal in Fe/MnAs/GaAs(001)

L. Lounis, M. Eddrief, M. Sacchi, F. Vidal

► **To cite this version:**

L. Lounis, M. Eddrief, M. Sacchi, F. Vidal. Layer-sensitive magneto-optical Kerr effect study of magnetization reversal in Fe/MnAs/GaAs(001). *Applied Physics Letters*, 2017, 111 (23), pp.232403. 10.1063/1.5004248 . hal-01655601

HAL Id: hal-01655601

<https://hal.science/hal-01655601>

Submitted on 24 Apr 2023

HAL is a multi-disciplinary open access archive for the deposit and dissemination of scientific research documents, whether they are published or not. The documents may come from teaching and research institutions in France or abroad, or from public or private research centers.

L'archive ouverte pluridisciplinaire **HAL**, est destinée au dépôt et à la diffusion de documents scientifiques de niveau recherche, publiés ou non, émanant des établissements d'enseignement et de recherche français ou étrangers, des laboratoires publics ou privés.

Layer-sensitive magneto-optical Kerr effect study of magnetization reversal in Fe/MnAs/GaAs(001)

L. Lounis,^{1,2} M. Eddrief,¹ M. Sacchi,^{1,3} and F. Vidal¹

¹*Sorbonne Universités, UPMC Univ Paris 06, CNRS-UMR 7588, Institut des NanoSciences de Paris, F-75005, Paris, France*

²*Ecole Normale Supérieure, PSL Research University, 75231 Paris, France*

³*Synchrotron Soleil, L'Orme des Merisiers Saint-Aubin BP 48, 91192 Gif-sur-Yvette Cedex, France*

(Dated: 15 November 2017)

Fe/MnAs/GaAs(001), a prototypical system for thermally assisted magnetization reversal, is studied by magneto-optical Kerr effect measurements. The results show that it is possible to recover elemental sensitivity from magneto-optical measurements when both Kerr rotation (θ_K) and Kerr ellipticity (ϵ_K) are measured under the same conditions. Both Fe and MnAs magnetic cycles can be extracted from simple linear combinations of θ_K and ϵ_K cycles. The data analysis shows that the orientation of the Fe magnetization at remanence can be controlled through the temperature of the system as a result of the peculiar temperature dependent self-organized stripes pattern in MnAs/GaAs(001).

MnAs, a ferromagnetic metal at room temperature, has attracted considerable interest since the first demonstration of epitaxial integration on semiconducting substrates^{1,2}. In the bulk, MnAs displays a first order magneto-structural phase transition at 313 K from the α -phase (hexagonal, ferromagnetic) to the β -phase (orthorhombic, not ferromagnetic). When MnAs is epitaxied on GaAs(001), the α - β phase transition is perturbed and the two phases coexist between ~ 10 and 40°C in the form of a self-organized pattern of α and β stripes running along the hexagonal MnAs [0001] axis.²⁻¹¹ The pattern has a well-defined period, proportional to the film thickness. Due to the difference of lattice parameters of α -MnAs and β -MnAs, a modulation of the layer thickness occurs as depicted in Fig. 1. In the 10 - 40°C temperature region, the period remains constant and the α phase proportion decreases continuously from 1 to 0.

Recently, the potentialities of the MnAs/GaAs(001) system as a magnetically active template were explored.¹²⁻¹⁷ It was shown that the magnetization of the Fe overlayer can be controlled quasi-statically through a fine tuning of the temperature.¹²⁻¹⁶ It was also shown that the Fe magnetization reversal can be triggered locally by a single femtosecond laser pulse¹⁷. The principal features of the striped pattern of MnAs/GaAs(001) remain unaffected in Fe/MnAs/GaAs(001) except for a variation of the period.¹⁸ The mechanism at play in the reversal is illustrated in Fig. 1. Due to the modulation in height and magnetic properties related to the α - β striped pattern, the dipolar field at the surface will act on the Fe overlayer. The temperature dependent α / β phase fraction tunes the amplitude of the dipolar field, which eventually leads to a controlled reversal of the Fe layer magnetization. Up to now such a process has essentially been studied by means of x-ray spectroscopy techniques that rely on large scale facilities to provide the elemental selectivity necessary to disentangle the magnetic contributions from MnAs and Fe. Here, we demonstrate that it is possible to retrieve the magnetic contributions from

Fe and MnAs and to study the reversal of the magnetization as a function of the temperature using magneto-optical Kerr effect (MOKE) measurements at a single wavelength.

The Fe/MnAs/GaAs(001) heterostructure was grown by molecular beam epitaxy (MBE) as described in previous works. We just recall briefly the principal steps here. GaAs substrates were first deoxidized under As overpressure followed by a GaAs buffer layer growth in standard conditions. The growth of a 200 nm thick MnAs epilayer was performed under As rich conditions. The epitaxial relationship was checked by reflection high energy electron diffraction. MnAs displayed a single domain epitaxy from the beginning of the growth with $[0001]_{\text{MnAs}} \parallel [1\bar{1}0]_{\text{GaAs}}$. Such epitaxy leads to stripes formation and guarantees that the easy magnetic axis of MnAs is parallel to $[110]_{\text{GaAs}}$ as schematized in Fig. 1(a). After UHV transfer to a dedicated MBE chamber, a 3 nm thick Fe layer was grown epitaxially on MnAs.¹⁵ The sample was capped with a protective, transparent and non-magnetic 5 nm thick ZnSe layer.

MOKE measurements were performed using a home-built set up composed of a polarized laser diode ($\lambda=450$ nm), Glan polarizers (rejection better than 10^5), a photoelastic modulator (modulation frequency $f=50$ kHz), a lock-in and an air cooled electromagnet ($H_{max}=5$ kOe) powered by a bipolar power supply. Data acquisition at f and $2f$ allows one to obtain signals proportional to the Kerr ellipticity ϵ_K and to the Kerr rotation θ_K , respectively.¹⁹ All magneto-optical measurements were performed in longitudinal configuration with the magnetic field applied along the MnAs easy magnetic axis, parallel to the sample surface and to the laser incidence plane. In such a geometry, MOKE is sensitive to the in-plane component of the magnetization that is parallel to the applied magnetic field. A Peltier thermoelectric device was used to vary the static sample temperature over the 10 - 40°C range, as monitored by a thermo-resistance. At each temperature T , ϵ_K and θ_K loops were recorded

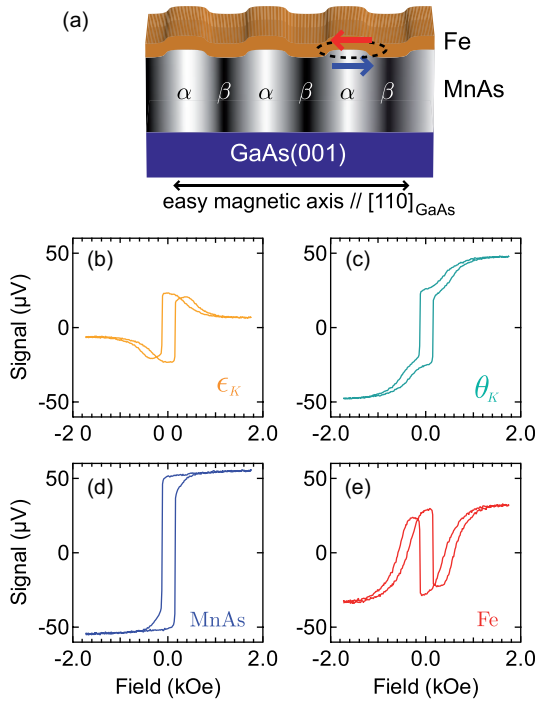


FIG. 1. (color online) (a) Schematics of the Fe/MnAs/GaAs(001) system in the temperature window leading to the α - β phase coexistence as a self-organized striped pattern. MnAs easy magnetic axis is oriented in the direction of the α - β modulation. The dashed curved line symbolizes the dipolar coupling leading to Fe magnetization reversal. (b-e) MOKE cyclic magnetometry of Fe/MnAs/GaAs(001) at $T=19^\circ\text{C}$. (b) Kerr ellipticity signal. (c) Kerr rotation signal. (d-e) MnAs and Fe signals retrieved from linear combination of signals displayed in (b) and (c), see text for details.

as a function of the magnetic field H .

Previous experimental reports and model calculations have shown that it is possible, under appropriate conditions, to achieve depth resolution by using MOKE to study magnetic multilayers.²⁰⁻²⁵ In the case of magnetic bilayers, with or without a non-magnetic spacer, Višňovský *et al.* have shown that the longitudinal MOKE response can be written as a linear combination of the individual contributions.²³ This is indeed valid in the case of an ultrathin magnetic layer on a magnetic substrate, as verified here. In the present case, labeling $S(\epsilon_K)$ the signal recorded at f and $S(\theta_K)$ the signal recorded at $2f$, we have:²³

$$S(\epsilon_K) = a_\epsilon^{Fe} M_\ell^{Fe} + a_\epsilon^{MnAs} M_\ell^{MnAs} \quad (1)$$

$$S(\theta_K) = a_\theta^{Fe} M_\ell^{Fe} + a_\theta^{MnAs} M_\ell^{MnAs} \quad (2)$$

M_ℓ^{Fe} and M_ℓ^{MnAs} are the longitudinal components of the magnetization and a_ϵ^{Fe} , a_ϵ^{MnAs} , a_θ^{Fe} and a_θ^{MnAs} are

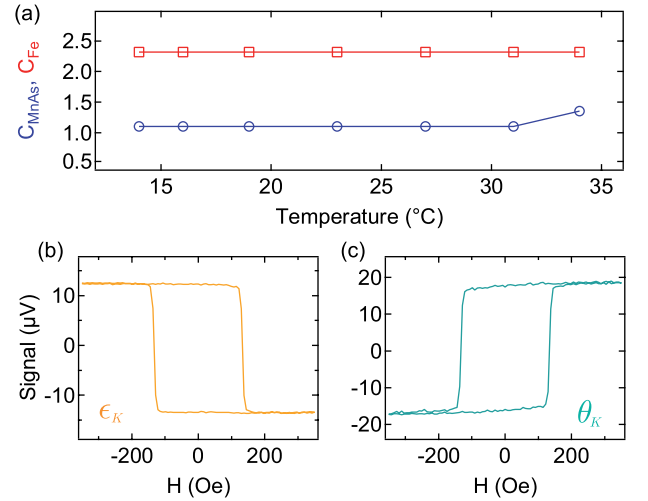


FIG. 2. (color online) (a) Variation of the c_{Fe} (squares) and c_{MnAs} (circles) coefficients as a function of the temperature. (b-c) ϵ_K and θ_K MOKE cycles of Fe/MnAs/GaAs(001) at $T=40^\circ\text{C}$.

coefficients that depend on optical constants, layer thicknesses and geometry. If equations 1 and 2 are verified, it is then possible to retrieve the contributions of the individual magnetic layers from a simple linear combination of $S(\epsilon_K)$ and $S(\theta_K)$, as:

$$M^{Fe} \propto S(\theta_K) - c_{Fe} S(\epsilon_K) \quad (3)$$

$$M^{MnAs} \propto S(\theta_K) + c_{MnAs} S(\epsilon_K) \quad (4)$$

Equations 3 and 4 can indeed be applied to the case of Fe/MnAs/GaAs(001). Fig. 1 shows measurements performed at $T=19^\circ\text{C}$ in the temperature window corresponding to the α - β phase coexistence. Clearly, the signals in Fig. 1(b-c) can be viewed as linear combinations of two cycles, one square and one slanted. In the case of ϵ_K , the two components have opposite signs, while for θ_K the combination is additive. The results of linear combinations following eqs. (3) and (4) are displayed in Fig. 1(d-e), using $c_{Fe}=2.32$ and $c_{MnAs}=1.1$. These coefficients can be adjusted in order to obtain a square loop for MnAs and the characteristic \mathcal{N} -shaped loop of Fe when α and β coexist in the sample as it was already measured by element-selective techniques using synchrotron radiation.¹⁶

ϵ_K and θ_K were measured in the 10-40°C range and the same procedure as described above was used in order to extract the magnetic cycles of Fe and MnAs. Over this temperature range, we did not observe any significant variations of c_{Fe} and c_{MnAs} , see Fig.2(a). At 40°C, similar responses are obtained for ϵ_K and θ_K except for the sign, as shown in Fig. 2(b-c). This is due to the fact that the whole MnAs film has transformed into the

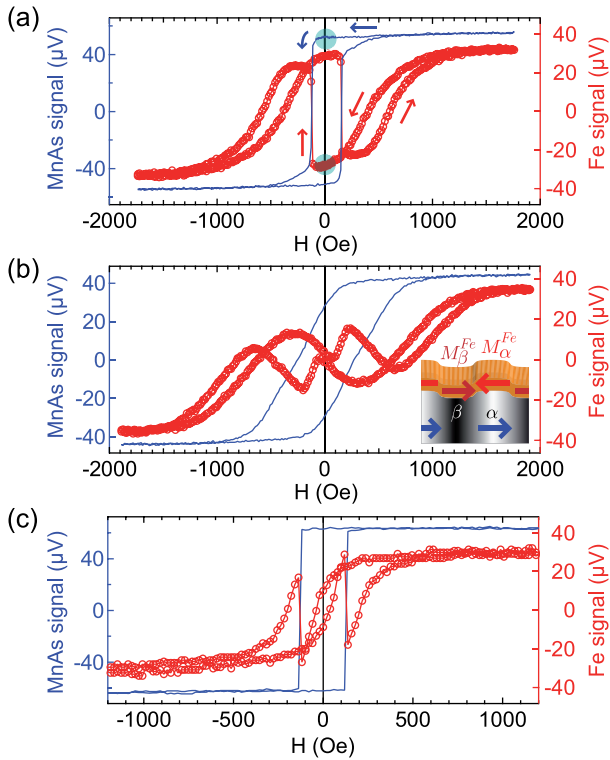


FIG. 3. (color online) (a) Layer-sensitive MOKE loops of Fe/MnAs/GaAs(001) at $T=19^\circ\text{C}$. Circles: Fe loop, line: MnAs loop. Arrows indicate the sense of the field variation. Shaded areas, corresponding to the same point of the field cycle, highlight the antiparallel Fe and MnAs magnetizations at remanence. (b) Same as (a) for $T=27^\circ\text{C}$. Inset: sketch of the magnetic configuration at remanence at $T=27^\circ\text{C}$. M_i^{Fe} with $i = \alpha, \beta$ denotes the Fe magnetization in regions located above phase i of MnAs. (c) Same as (a) for $T=10^\circ\text{C}$.

β -phase and does not contribute anymore to the ferromagnetic response. Thus, at 40°C , only the contribution of Fe is observed and a square loop, unaffected by any coupling with the underlying layer, is obtained.

We note that element selectivity can be achieved in transition metal (TM)-rare earth (RE) compounds by measuring at different wavelengths of the laser probe.^{26–28} In FeTb and TbCo compounds, for instance, it was shown that 780 nm radiation provides sensitivity to the TM magnetization, whereas 390 nm probes mainly the Tb magnetization.^{26,28} This method, though, relies on the very different magneto-optical response of RE at near ultraviolet wavelengths that can excite the $4f$ electrons and cannot be extended to TM-TM compounds. In our experiment we verified that using a 650 nm wavelength yielded also $S(\epsilon_K)$ and $S(\theta_K)$ signals that are linear combinations of M_ℓ^{MnAs} and M_ℓ^{Fe} .

Although our analysis could be guided by the available element selective synchrotron data, MOKE measurements are self-sufficient for a unique determination of the c_{Fe} and c_{MnAs} coefficients. Indeed, at low temperature, where MnAs is in the pure α phase, there

is no dipolar coupling acting on Fe and the two layers feature square uncoupled hysteresis loops. Moreover, at high temperature MnAs is in the β phase and only the Fe layer is ferromagnetic. Therefore, layer-sensitive MOKE, a relatively simple technique available in the laboratory, can be a valuable complementary technique to element-specific measurements based at large scale facilities. It should be noted that the method can be applied to layered systems with magnetic coupling of distinct nature (exchange, dipolar, exchange-bias).^{25,29} In this respect, it may be applied to Co/FeRh bilayers in order to study the temperature-dependent coupling arising from the antiferromagnetic-ferromagnetic phase transition in FeRh.³⁰ Concerning the limitations of the technique, it should be noted that, if it works well for the acquisition of magnetic cycles, temperature or time dependent measurements with layer resolution can be more involved and element-selectivity remains a major asset.

Having validated the use of MOKE for obtaining layer selectivity, we now discuss the results obtained as a function of the temperature. Measurements were performed in the $10\text{--}40^\circ\text{C}$ range for increasing (after cooling at 5°C , pure α phase) and decreasing (after heating at 45°C , pure β phase) temperatures. Fig 3(a) shows Fe and MnAs cycles obtained at 19°C . The \mathcal{N} -shaped loop of Fe can be explained as follows: starting at positive saturation, H overcomes the MnAs generated dipolar field and both layers have their magnetization pointing in the same direction. While lowering H , the effect of the dipolar field becomes progressively more relevant, till the Fe magnetization turns antiparallel to that of MnAs, as illustrated at remanence in Fig. 1(a). When, after sign inversion, H matches the MnAs coercive field and reverses its magnetization, the sign of the dipolar field reverses as well, dragging the Fe magnetization and maintaining the antiparallel alignment of the two layers. Finally, when H approaches the negative extreme of the loop it overcomes again the dipolar field and turns the Fe and MnAs magnetizations parallel. At $T=27^\circ\text{C}$, one has the same behavior, except in the vicinity of $H=0$ where a sharp variation of the Fe signal is observed, see Fig 3(b). This signal nearly vanishes at $H=0$. We interpret this reduction of the remanent magnetization of Fe, M_r^{Fe} , as the consequence of the decreasing of the α/β ratio as the temperature increases. Indeed, for equal proportion of α and β , only the fraction of Fe located above α -MnAs will see its magnetization M_α^{Fe} reversed. In contrast, M_β^{Fe} will remain unaffected, as shown schematically in the inset of Fig. 3(b). This explains why the average Fe magnetization is close to zero at temperatures for which the α and β fractions closely match. At lower temperature, a parallel configuration of Fe and MnAs magnetization is recovered, as shown in Fig. 3(c), this will be further discussed in what follows.

Fig. 4(a-b) show the evolution of the MnAs magnetic cycles and remanent magnetization as a function of the temperature. Due to the increasing β fraction in the system, both the remanent and saturation magnetiza-

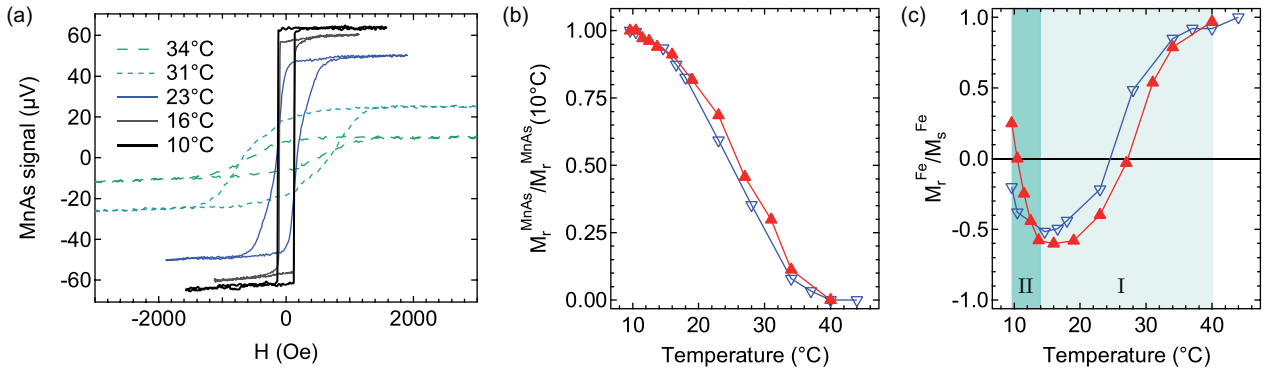


FIG. 4. (color online) (a) MnAs magnetic cycles in the α - β phase coexistence T range. (b) MOKE derived MnAs remanent magnetization as a function of temperature, normalized to 1 at $T=10^\circ\text{C}$. (c) Fe remanent to saturation magnetization ratio as a function of the temperature. In (b) and (c) the filled and open symbols indicate increasing and decreasing temperatures, respectively. Temperature ranges labeled I and II correspond to α - β phase coexistence as a striped pattern and to the coexistence of α - β stripes with pure α regions, respectively.

tion of MnAs decrease when the temperature increases. The evolution of the magnetic response of MnAs with increasing temperature is similar to the one observed in the absence of a Fe overlayer. The results shown in Fig. 4(b) are consistent with a phase coexistence in the 10-40°C range. The first order character of the α - β phase transition is apparent from the thermal hysteresis in Fig. 4(b). It was shown in a previous study that the presence of the Fe overlayer affects the total elastic energy of the system, leading to a change in the period of the α - β stripes pattern.¹⁸ In contrast, the extension of the coexistence range and the critical temperature remain unaffected. The evolution of the coercive field H_c with the temperature confirms the fact that the Fe overlayer has little impact on MnAs magnetic properties: H_c tends to increase with temperature, mainly because of the α stripes narrowing that favors complex magnetic structures with out-of-plane magnetization domains.^{31,32} This is also the general trend we observed in our samples.¹²

The remanent magnetization of Fe does not exhibit a monotonic behavior. Fig. 4(c) shows the evolution of the $M_r^{\text{Fe}}/M_s^{\text{Fe}}$ ratio, M_s^{Fe} being the saturation magnetization of Fe, as a function of the temperature. A salient feature of this evolution is that $M_r^{\text{Fe}}/M_s^{\text{Fe}}$ changes sign in the temperature range corresponding to the α - β phase coexistence [region I in Fig. 4(c)]. The ratio is negative for T below 27°C and positive above this temperature. At $T=40^\circ\text{C}$, the ratio is close to 1, which is expected because only Fe is ferromagnetic at this temperature [see Figs. 3(b-c)] and the stripes pattern has disappeared. Let us label Fe^α the portions of Fe film above α -MnAs and Fe^β the portions of Fe film above β -MnAs at a given temperature. For temperatures comprised between 27°C and 40°C , Fe^β dominates over Fe^α , explaining the positive sign of $M_r^{\text{Fe}}/M_s^{\text{Fe}}$. At $T=27^\circ\text{C}$, the ratio $M_r^{\text{Fe}}/M_s^{\text{Fe}}$ is close to zero as a consequence of Fe^α and Fe^β having equal proportions. For $T \leq 27^\circ\text{C}$, Fe^α dominates and the sign of M_r^{Fe} is reversed. It is interesting to notice that

there is a minimum in $M_r^{\text{Fe}}/M_s^{\text{Fe}}$ around 19°C . This can be understood as follows: the formation of an efficient dipolar field at the Fe/MnAs interface requires the formation of α - β stripes, favoring the reversal of Fe. At the same time, the fraction of reversed Fe scales as the fraction of Fe^α . This leads to the existence of an optimal temperature for the fractional Fe reversal at remanence. At lower temperatures, as shown in region II of Fig. 4(c), the fraction of reversed Fe drops and M_r^{Fe} eventually becomes positive [see Fig. 3(c)]. This corresponds to a temperature range where the coexistence of pure α and α - β stripes regions has been previously reported.³³ The dipolar coupling vanishes in pure α regions, therefore $M_r^{\text{Fe}}/M_s^{\text{Fe}}$ tends to change sign in region II as a consequence of the coexistence of α - β stripes and pure α regions.

In conclusion, we studied the Fe/MnAs/GaAs(001) system by magneto-optical Kerr effect measurements, demonstrating the possibility to extract the magnetic cycles of Fe and MnAs from simple linear combinations of Kerr ellipticity and Kerr rotation loops acquired under the same conditions. Thanks to the layer sensitivity of the technique, a detailed picture of the magnetization reversal can be established, evidencing an optimal temperature for Fe reversal in the α - β phase coexistence region of MnAs.

ACKNOWLEDGMENTS

We thank F. Breton for the development of the control software of the MOKE set-up and R. Delaunay, G.S. Chiuzaian, B. Vodungbo, M. Marangolo, V. H. Etgens and Y. Zheng for useful discussions.

¹M. Tanaka, J. P. Harbison, T. Sands, T. L. Cheeks, V. G. Keramides, G. M. Rothberg, J. Vac. Sci. Technol. B **12**, 1091 (1994).

²L. Däweritz, Rep. Prog. Phys. **69**, 2581 (2006).

- ³V. M. Kaganer, B. Jenichen, F. Schippan, W. Braun, L. Däweritz, and K. H. Ploog *Phys. Rev. B* **66**, 045305 (2002).
- ⁴C. Adriano, C. Giles, O. D. D. Couto, M. J. S. P. Brasil, F. Iikawa, L. Däweritz, *Appl. Phys. Lett.* **88**, 151906 (2006).
- ⁵M. Kästner, C. Herrmann, L. Däweritz, K. H. Ploog, *J. Appl. Phys.* **92**, 5711 (2002).
- ⁶T. Plake, M. Ramsteiner, V. M. Kaganer, B. Jenichen, M. Kästner, L. Däweritz, K. H. Ploog, *Appl. Phys. Lett.* **80**, 2523 (2002).
- ⁷M. Kästner, F. Schippan, P. Schützendübe, L. Däweritz, K. H. Ploog, *J. Vac. Sci. Technol. B* **18**, 2052 (2000).
- ⁸R. Magalhães-Paniago, L. N. Coelho, B. R. A. Neves, H. Westfahl, F. Iikawa, L. Däweritz, C. Spezzani, M. Sacchi, *Appl. Phys. Lett.* **86**, 053112 (2005).
- ⁹F. Vidal, O. Pluchery, N. Witkowski, V. Garcia, M. Marangolo, V. H. Etgens, Y. Borensztein, *Phys. Rev. B* **74**, 115330 (2006).
- ¹⁰B. Gallas, J. Rivory, H. Arwin, F. Vidal, M. Stchakovsky, *Phys. Stat. Solidi (a)* **205**, 863 (2008).
- ¹¹R. Breitwieser, F. Vidal, I. L. Graff, M. Marangolo, M. Eddrief, J.-C. Boulliard, and V. H. Etgens, *Phys. Rev. B* **80**, 045403 (2009).
- ¹²M. Sacchi, M. Marangolo, C. Spezzani, L. Coelho, R. Breitwieser, J. Milano, V. H. Etgens, *Phys. Rev. B* **77**, 165317 (2008).
- ¹³R. Breitwieser, M. Marangolo, J. Lüning, N. Jaouen, L. Joly, M. Eddrief, V. H. Etgens, M. Sacchi, *Appl. Phys. Lett.* **93**, 122508 (2008).
- ¹⁴M. Sacchi, M. Marangolo, C. Spezzani, R. Breitwieser, H. Popescu, R. Delaunay, B. Rache Salles, M. Eddrief, and V. H. Etgens, *Phys. Rev. B* **81**, R220401 (2010).
- ¹⁵C. Helman, J. Milano, S. Tacchi, M. Madami, G. Carlotti, G. Gubbiotti, G. Alejandro, M. Marangolo, D. Demaille, V. H. Etgens, and M. G. Pini, *Phys. Rev. B* **82**, 094423 (2010).
- ¹⁶C. Spezzani, F. Vidal, R. Delaunay, M. Eddrief, M. Marangolo, V. Etgens, H. Popescu, and M. Sacchi, *Sci. Rep.* **5**, 8120 (2015).
- ¹⁷C. Spezzani, E. Ferrari, E. Allaria, F. Vidal, A. Ciavardini, R. Delaunay, F. Capotondi, E. Pedersoli, M. Coreno, C. Svetina, L. Raimondi, M. Zangrando, R. Ivanov, I. Nikolov, A. Demidovich, M. B. Danailov, H. Popescu, M. Eddrief, G. De Ninno, M. Kiskinova, and M. Sacchi, *Phys. Rev. Lett.* **113**, 247202 (2014).
- ¹⁸F. Vidal, C. Spezzani, R. Breitwieser, M. Marangolo, M. Eddrief, M. Sacchi, and V. Etgens, *Appl. Phys. Lett.* **97**, 251914 (2010).
- ¹⁹K. Sato, *Jpn. J. Appl. Phys.* **20**, 2403 (1981).
- ²⁰M. R. Puffall, C. Platt, and A. Berger, *J. Appl. Phys.* **85**, 4818 (1999).
- ²¹S. Maat, L. Shen, C. Hou, H. Fujiwara, and G. J. Mankey, *J. Appl. Phys.* **85**, 1658 (1999).
- ²²I. Sveklo, Z. Kurant, A. Maziewski, E. Sieczkowska, A. Petrouchik, L. T. Baczewski, A. Wawro, *J. Magn. Magn. Mater.* **345**, 82 (2013).
- ²³S. Višňovský, K. Postava, T. Yamaguchi, and R. Lopusník, *Appl. Optics* **41**, 3950 (2002).
- ²⁴J. Hamrle, J. Ferré, M. Nývlt, and Š. Višňovský, *Phys. Rev. B* **66**, 224423 (2002).
- ²⁵P. Vavassori, V. Bonanni, A. Busato, D. Bisero, G. Gubbiotti, A. O. Adeyeye, S. Goolaup, N. Singh, C. Spezzani, and M. Sacchi, *J. Phys. D: Appl. Phys.* **41**, 134014 (2008).
- ²⁶A.R. Khorsand, M. Savoini, A. Kirilyuk, A. V. Kimel, A. Tsukamoto, A. Itoh, and T. Rasing, *Phys. Rev. Lett.* **110**, 107205 (2013).
- ²⁷Y. Tsema, M. Savoini, A. Tsukamoto, A. V. Kimel, A. Kirilyuk, and T. Rasing, *Appl. Phys. Lett.* **109**, 172403 (2016).
- ²⁸S. Alebrand, U. Bierbrauer, M. Hehn, M. Gottwald, O. Schmitt, D. Steil, E. E. Fullerton, S. Mangin, M. Cinchetti, and M. Aeschlimann, *Phys. Rev. B* **89**, 144404 (2014).
- ²⁹S.-K. Kim, J.-W. Lee, S.-C. Shin, and K. Y. Kim, *J. Appl. Phys.* **91**, 3099 (2002).
- ³⁰L. Lounis, C. Spezzani, R. Delaunay, F. Fortuna, M. Obstbaum, S. Günther, C. H. Back, H. Popescu, F. Vidal, and M. Sacchi, *J. Phys. D: Appl. Phys.* **49**, 205003 (2016).
- ³¹T. Plake, T. Hesjedal, J. Mohanty, M. Kästner, L. Däweritz, and K. H. Ploog, *Appl. Phys. Lett.* **82**, 2308 (2003).
- ³²R. Engel-Herbert, J. Mohanty, A. Ney, T. Hesjedal, and L. Däweritz, *Appl. Phys. Lett.* **84**, 1132 (2004).
- ³³A. Ney, T. Hesjedal, C. Pampuch, A. K. Das, L. Däweritz, R. Koch, K. H. Ploog, T. Toliński, J. Lindner, K. Lenz, and K. Baberschke, *Phys. Rev. B* **69**, 081306(R) (2004).